Study of Two-Phase Flow for a Ramjet Combustor

D. Laredo,* Y. Levy,† and Y. M. Timnat‡
Technion—Israel Institute of Technology, Haifa 32000, Israel

A reactive two-phase flow is studied experimentally by a special laser Doppler anemometry (LDA) technique and numerically by solving the elliptic governing equations. The relation between the liquid fuel injection and the aerodynamic flameholding mechanism of a dump combustor was investigated. The flow geometry chosen was an axisymmetric sudden expansion with small diameter ratio. The measurements included pressure, temperature, gas species concentration, as well as velocities of both phases and droplet size. A special processing technique enabled the simultaneous measurement of the gas velocity represented by the smallest droplets and of the size-velocity correlation of the droplets in the range of 5–500 μm. The specific geometry of the sudden expansion combustor creates an annular flame stabilized just downstream of the step. The geometry of the flame depended very much on the equivalence ratio, with larger values creating longer and thicker flames. The combustion shortened the recirculation length from about 11 times the step height to about four times. There was no direct influence of the droplets on the average gas velocity in cold flow, whereas the size distribution of the droplets had significant influence on the combusting flow pattern. Two computational case studies were performed for isothermal and reactive two-phase flow situations. The numerical results indicated the fast dynamic and thermal response of the small droplets to the surrounding gas flow. Moreover, the droplets did not penetrate into the fuel-rich recirculation zone. The shear layer, which separates it from the core, was characterized by a local equivalence ratio close to unity. The numerical predictions and the experimental results exhibited fairly good agreement, provided that the initial conditions of the spray and the thermal boundary conditions are determined experimentally.

I. Introduction

TURBULENT shear flows with recirculation can enhance and improve stabilization of flames in air-breathing engines. The aerodynamics of recirculating flows in conjunction with the spray dynamics of the fuel droplets determines the distribution of the fuel, and the various flow regions create stable burning zones within the combustor.[1]

Numerous efforts are currently under way using computational and experimental techniques[2] to increase the understanding of the complex flowfields and to predict and control the specific stabilized zones.

The common combustor configuration mostly investigated is that of confined coaxial swirl stabilized flames, typically used in gas turbines, boilers, furnaces, and incinerators.[3] The dump combustor configuration (without flameholders) chosen in this study is more suitable for integral rocket ramjets and after burners.[4] The former configuration has the advantage of being able to burn heavier fuels and to work at higher equivalence ratios, while the dump combustor is better suited to aircraft engines due to its potentially lower pressure drop and simplicity in design. The specific flow in dump combustors presents several complex features due to the recirculation region, which can be used advantageously as a flameholder.

In this region, the mean velocities are low and the flow is highly turbulent. The establishment of the recirculating zone can be described as follows: the flow behaves initially like a sudden (free) expansion up to the stage where the jet becomes attached to the chamber walls. However, unlike the free expansion, there is a limited supply of gases to provide free shear-layer entrainment, so that a reduction in pressure must occur behind the rearward facing step, resulting in an upstream movement of the reattachment point. The freestream flow and the recirculation vortex interacting with a jet of trailing eddies of the mixing layer enhance the interaction between combustion products and reactants and act locally as a heat exchanger. The geometry of the flame front is strongly dependent on the turbulent flowfield, affected by the accelerated mixing parameters and by the hot gases expansion, which results in the reduction of the recirculation zone length. The geometry and the influencing parameters of the recirculating regions (working conditions, phenomenological parameters) were studied by several workers. Stevenson et al.[5] state that, based on a review of experimental results, the reattachment length in cold flow varies between six and 11 step heights. They suggest that the variations in the measurements is essentially due to an adverse pressure effect and not to the differences in the inlet conditions. They pointed out the high turbulence level on the combustor centerline indicating that the flow downsteam of the reattachment point is still carrying the large-scale eddies. The combustion decreases the recirculation zone length by 10–30%, probably due to the expansion of the gases. The discrepancies in the influence of combustion are still to be investigated due to the lack of sufficient experimental results.

The development of laser diagnostic techniques has offered the possibility for more accurate measurements of mean and fluctuating properties in combustion flows. Advanced laser anemometry enables two-phase flow measurements, i.e., size-velocity correlation of the liquid droplets and the gas velocity.[6] Moreover, a newly developed technique, the phase Doppler anemometry,[7,8] augments the accuracy of the droplet size measurement. In two-phase flows signals are obtained simultaneously from both phases. Particles of all sizes are detected, those in the low range serve as tracking particles and represent the continuum phase. The particle velocity is linearly related to the Doppler frequency and their size is connected to the signal amplitude in the so-called pedestal technique. Because of the spatial distribution of the light within the control volume of the laser probe, the droplet signal is also related to its path. To overcome this size bias, several techniques are suggested (off-axis detection, simultaneous or-

Received Oct. 16, 1989; revision received June 20, 1990; accepted for publication Sept. 12, 1990. Copyright © 1990 by the American Institute of Aeronautics and Astronautics, Inc. All rights reserved.

*Faculty of Aerospace Engineering and Space Research Institute; currently, Research Associate, Naval Postgraduate School, Monterey, CA.

†Senior Lecturer, Faculty of Aerospace Engineering and Space Research Institute.

‡Professor, Faculty of Aerospace Engineering and Space Research Institute. Associate Fellow AIAA.

thogonal detection, and electronic segregation). The principle of the phase Doppler anemometry is to relate the droplet size to a phase shift between two or more detected signals; hence, it practically requires three photodetectors and special signal processing.

II. The Experiment

A. Geometry

The model combustor configuration presented in Fig. 1 includes the features required of practical combustors. It consists of an 80-mm i.d. cylindrical quartz tube extending 35 cm from the plane of the step. The air is introduced through a tube including a flow straightener with inlet diameters of 53 mm or 40 mm which results in abrupt diameter expansion ratios of 1.5 and 2. The combustor is operated at atmospheric pressure. The fuel (kerosene) is introduced through a hollow (optionally a full) cone liquid spray nozzle centrally mounted at 25 cm before the inlet plane. The airflow velocity was varied from 30–50 m/s and the overall equivalence ratios considered for reacting conditions were $\phi = 0.2$ and $\phi = 0.3$.

B. Size-Velocity Measurements

Axial, mean, and rms velocity and droplet size measurements are performed using an LDA optical system (DISA 55X unit). The beam from a 15-mW He-Ne laser (Spectra Physics 120) is split into two beams of equal intensity 60 mm apart. A 40-MHz frequency shift is applied to one of the beams in order to avoid directional ambiguity. The beams are then focused through a 300-mm lens to form the measuring volume located within the test section. This arrangement results in a set of interference fringes spaced at 3.3 μm apart, sensitive to the axial velocity component. The receiving optics consist of a 250-mm lens focused onto a 0.1-mm-diam photomultiplier tube aperture. The dimensions of the probe volume obtained are about 190 μm in diameter with a length of 1.8 mm. However, due to the requirement imposed by the processing electronics presented in the next section, the effective length is slightly less than 1.2 mm. The principle of the size-measurement technique is based on the almost linear relation between the diameter of the fuel droplets and the maximum amplitude (pedestal value) of the signal as detected by the photomultiplier.[9,10] Although the pedestal technique has an inherent disadvantage (need for a calibration curve and dependence of the scattered light intensity on the droplet path within the probe volume), its attractiveness is due to the large dynamic range and the simpler method required for automatic data acquisition. The fuel droplets originated from the spray nozzle are used as the seeding particles for the LDA system. Small oil droplets (less than 5 μm) are added, in the nonreactive flow, in order to measure gas velocity specifically relevant in the complex regions such as near the walls under the recirculation zone. A special processing technique enables the simultaneous measurement of the gas velocity, represented by the smallest droplets, and of the size-velocity correlation of the droplets (in the range of 5–500 μm).

C. Data Acquisition and Processing

The electrical signal generated by the photomultiplier enters two parallel branches for simultaneous measurements of the Doppler frequency and the pedestal amplitude.

The Doppler

The signal from the photomultiplier is connected via a 20-db amplifier (RF-H102L) to a Doppler frequency processor (TSI Model 1980b) directly or, when frequency shift is applied, through a high-pass filter and an electronic mixer (DISA model 55 N 10). The 1-MHz high-pass filter (TTE Inc., USA, Model H67E with a cutoff frequency of 100 MHz) acts as a buffer between the photomultiplier and the mixer. The filter prevents reverse influence of the mixer on detected signals, which may cause significant deterioration of their shape, precluding the possibility of obtaining reliable pedestal amplitude measurements. The electronic mixer combines the signal from the photomultiplier with an internally selected frequency to form an effective frequency shift between 0.01 and 9 MHz. The frequency counter converts the frequency to a linearly related analog voltage.

The Pedestal Amplitude Branch

In order to obtain the pedestal amplitude, the signal from the photomultiplier is connected to a low-pass filter (TTE M0047, 3 MHz) that removes the Doppler frequency oscillation revealing the pedestal amplitude of the signal. The signal is then directed to a specially built peak detector.[6] The timing diagram of the peak detector operation, depicted in Fig. 2, shows that it maintains the pedestal amplitude until a new signal appears. It is then reset to zero and follows the increase of the new signal up to it speak. It should be noted that all signals with amplitude higher than the trigger level are detected by the peak detector. This is not the case with the frequency counter where an internal signal-validation test is performed. It follows that the number of particles measured by the peak detector is much larger than for the counter.

Data Processing

The output results of the frequency count and the peak detector are in the form of a linear-related analog voltage. Both instruments are connected to an analog-to-digital (A/D) converter with a maximum sampling rate of 100 kHz and 12 bits resolution. Both signals are sampled sequentially by a multiplexer. Data are stored temporarily in the minicomputer (PDP 11/84) buffer memory and then processed and stored on hard disk.

The sequential sampling that is performed at a preselected and fixed rate is recorded in the computer memory as pairs of integers-corresponding to the Doppler frequency and the pedestal amplitude. The velocity and the pedestal amplitude information are obtained by performing a special validation test on all recorded values. The validation criteria were selected to ensure that the measured velocity and the associated pedestal amplitude belong to the same particle. The validation criteria are

$$\begin{bmatrix} |V_2/V_1 - 1| > \varepsilon \\ \text{and} \\ |V_3/V_2 - 1| < \varepsilon \end{bmatrix} \text{ and } \begin{bmatrix} \{|d_2/d_1 - 1| > \varepsilon \\ \text{and} \\ |d_3/d_2 - 1| < \varepsilon\} \text{ or } \{|d_3/d_2 - 1| > \varepsilon \\ \text{and} \\ |d_4/d_3 - 1| < \varepsilon\} \end{bmatrix}$$

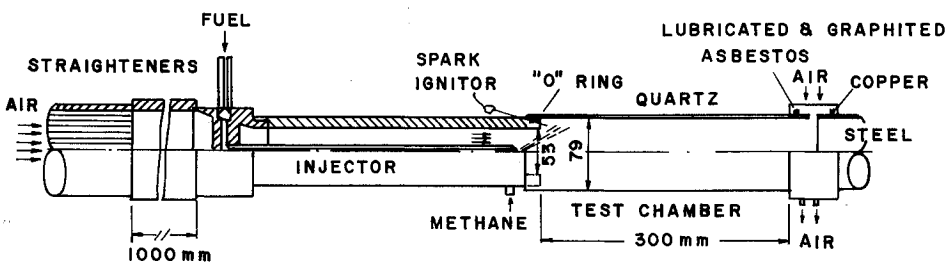

Fig. 1 The flow system and the dump combustor.

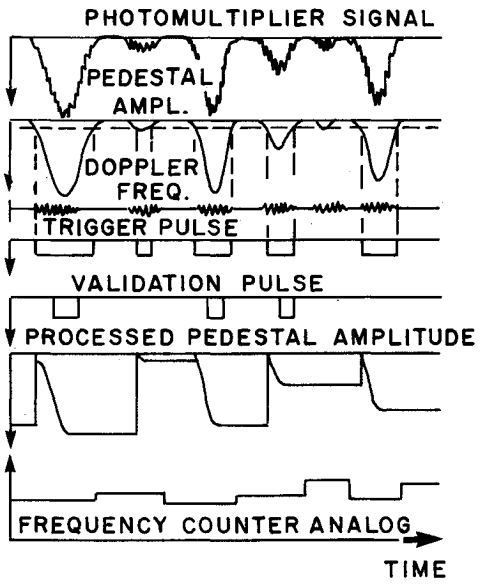

Fig. 2 Timing diagram for peak detector operation.

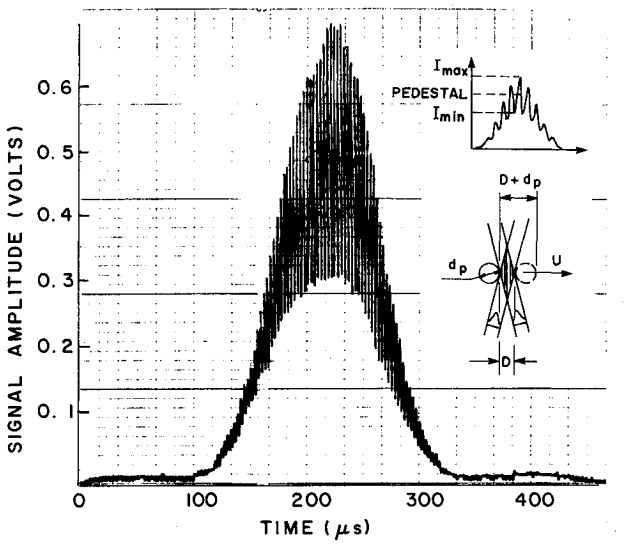

Fig. 3 Typical signal recorded from droplet during the calibration test.

where V_1, V_2, V_3 are the velocity values and d_1, d_2, d_3, d_4 are the pedestal amplitude values. ε is an accuracy factor depending on the noise level and has a typical value of 1%. If the validation test is passed, V_3 and d_3 represent the velocity and pedestal amplitude of a validated signal. Such pairs of data are used to perform ensemble averaging according to groups of similar pedestal amplitudes. For each group, the velocity mean and rms values are calculated and a velocity histogram is displayed.

D. Calibration Technique

A preliminary requirement for droplet sizing is a calibration test performed at conditions as similar as possible to the experimental ones. The effect of differences in operating conditions are difficult to evaluate and could lead to erroneous results.

In the calibration technique developed, a conventional syringe mounted vertically downwards is connected to a fuel tank pressurized at different levels, which produces a train of liquid droplets. The droplet diameter is affected by the pressure of the syringe and the needle diameter. The exact droplet diameter cannot be accurately predicted. The syringe is aligned so that the train of droplets crosses the control volume of the LDA system exactly at the center and in a direction perpendicular to the bisector of the incident laser beams. The droplets path is aligned by obtaining signals of maximum amplitude. Special attention is required not to reach saturation level at the photomultiplier due to the high light intensity scattered by the droplets.

The signals from the photomultiplier are recorded by a digitizer (Biomation Gould No. 2805) and then plotted on a recorder. A typical plot is shown in Fig. 3. The pedestal amplitude A_p, the duration of the signal ΔT, and the Doppler frequency (and so the velocity V) can be measured from the recorder plot. The diameter of the droplet is calculated using the relation

$$d_p + D = \Delta TV$$

where D is the effective control volume diameter. Values of pedestal amplitude $(D + d_p)$ are plotted for different droplet diameters thus giving a d_p vs A_p relation. A typical calibration curve is shown in Fig. 4. One must remember that the calibration curves and the values of effective control-volume diameter are applicable only to specific experimental conditions and therefore no universal calibration constants can be obtained.

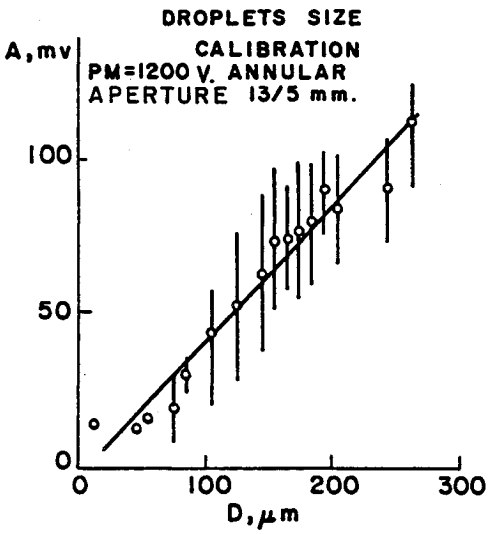

Fig. 4 Calibration of the scattered light to droplet-size correlation.

In order to overcome the ambiguity caused due to the different possible paths of the droplet within the control volume, several alternatives are possible, namely:

1) The use of photodiodes to identify electrooptically those droplets that pass through the central part of the control volume.

2) Side detection that restricts the view of the photomultiplier to the core of the control volume.

3) The request for a minimum number of fringes which is an indicator for the trajectory of the droplet. However, as this number is influenced by the frequency shift, special care should be given in considering this velocity-linked effect.

III. Numerical Method

Calculation of a flowfield with large regions of recirculation requires the solution of the elliptic form of the governing equations. The chosen turbulence model is the k-ε model for highly turbulent reactive flows based on the eddy viscosity concept.[11]

The combustion model adopted is the simple phenomenological one of Magnussen and Hjertagger[12] who made use of the eddy breakup model, which implies that the mean reaction rate is determined solely by the rate-of-scale reduction via a process of turbulent vortex stretching.

The trajectories of the liquid droplets, produced by the spray atomizer, were calculated as they traversed the gaseous flowfield. This method involves the adaptation of the droplets equations of motion, written in Lagrangian form, into the Eulerian gas-phase equations. The liquid-phase model represents the spray by individual droplets.[13] Each computational droplet represents a group of similar droplets, all having identical initial size and velocity.

The droplet source terms are obtained by calculating the loss or gain of droplet mass, momentum, and energy within each computational cell of the Eulerian finite-difference grid through which the droplet passes (PSIC method). The net difference of particle properties between those entering and leaving a given cell provides the liquid-phase source terms. The drop dispersion by turbulence and the effects of the turbulence on the interphase transport rates are ignored. Moreover, the droplets are assumed to interact only with the mean gas motion and they do not interact with each other. In the calculation of the momentum transfer, the model employs the standard drag coefficient for spheres and ignores other forces (e.g., Basset force). Also, the work of the interphase forces in the energy source term is ignored. These approximations are appropriate for high void fractions and high liquid-to-gas density ratios.[13] The overall solution is obtained by iterating between the calculations of the two phases until convergence is reached.[14] The program has two convergence cycles, an internal one for the gas phase and an "outer" one for the liquid phase. The gaseous phase will converge when the sum of errors from all numerical cells will be less than 0.5% and final convergence will occur when the droplet trajectories will exhibit a cumulative error of less than 0.1%. A nonlinear grid of 22/22 required about 8900 s of the IBM 301D CPU.

IV. Experimental Results

In order to understand the two-phase flow phenomena, both cold and reactive experiments were performed inside the dump combustor. The fuel nozzle was characterized in free and confined environments. The droplet size and axial velocity were measured together with the surrounding gas flow. The gas temperature and composition were also measured together with the wall pressure for a quick indication of the recirculation length.

A. Cold Flow

Figure 5 displays radial profiles of the axial gas velocity at different cross sections along the combustor with a flow rate of 0.175 kg/s and an expansion ratio of $D/d = 1.5$. The profiles clearly show the drastic reduction from about 40 m/s to zero just opposite the edge of the expansion step. Further downstream the profile displays a much smoother curve, where the zero velocity value is much closer to the tube wall. The negative velocity values clearly demonstrate the existence of the recirculation zone downstream of the expansion plane. It should be noted that the slight reduction at the center of the profile is actually the wake of the spray nozzle located upstream. The turbulent intensity is of the order of 30%. However, in the recirculation zone the fluctuation component can exceed considerably the local average velocity. A quick and convenient way to measure the length of the recirculation zone was achieved by using an oil coating on the inner zone tube side. The reverse flow region can be easily distinguished and measured. Using such a technique, the length of the recirculation zone was found as a function of the Reynolds number Re. It was found that while changing the flow rate by a factor of 2.5 ($Re = 2 \times 10^4$–5×10^4) the length of the (normalized) recirculation zone changed only by about 20% (from 11 to 9 times the step height).

The fuel droplets are injected at relative low velocities (about 20 m/s), whereas the air penetrates the combustor at about 50–70 m/s. As the injector is located just upstream of the step, the air velocity adjacent to it is the highest and the droplet will accelerate to values close to those of the air. The

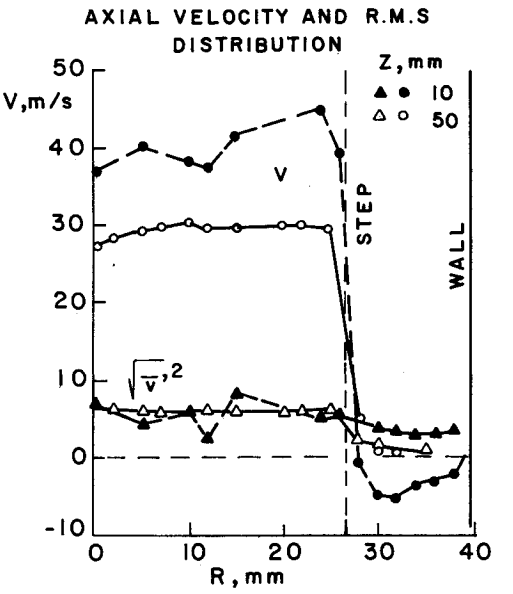

Fig. 5 Radial distribution of the mean axial velocity and of the turbulence at 10 and 50 mm from the entrance ($D/d = 1.5$; $m_{air} = 175$ g/s).

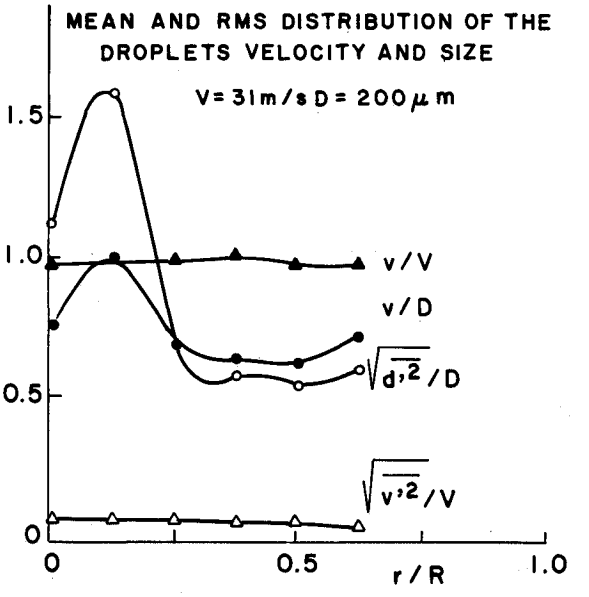

Fig. 6 Radial distribution of: 1) normalized droplet mean axial velocity; 2) turbulence intensity; 3) mean size; and 4) normalized variance of the droplet size (cold flow).

small drops are the most sensitive to the air velocity gradients and will exhibit similar velocity distributions. However, the large droplets will exhibit smoother profiles, due to their larger inertia. The normalized radial distribution of the droplet mean and rms velocities and diameters are given in Fig. 6 (the maximum mean diameter was about 200 μm and the maximum mean axial velocity was 31 m/s). The large standard deviation in the droplet size indicates the spread of the droplet diameters, which is of the order from zero to about 150% the mean value.

B. Reactive Flows

The specific geometry of the sudden expansion combustor creates a ring-shaped flame, stabilized just downstream of the step. The geometry of the flame depended very much on the equivalence ratio (apart from the Re number) with larger values creating longer and thicker flames. Figure 7 clearly demonstrates the influence of combustion on the recirculation length. It is seen that combustion shortens it from about 11 times the step height to about only four times. Figure 8 shows

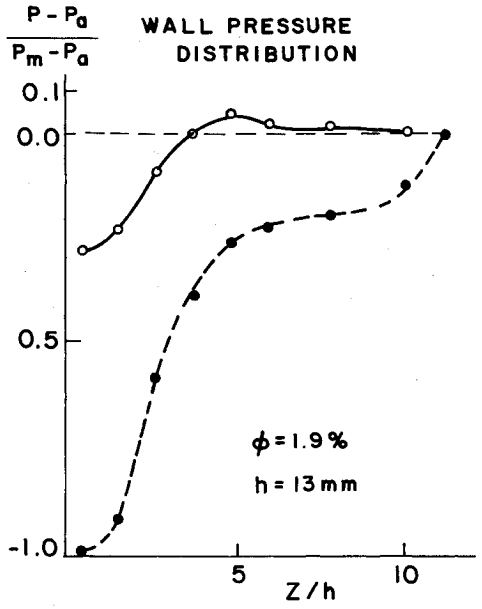

Fig. 7 Static pressure distribution along the combustor wall in cold and reactive flow, — reactive flow, --- cold flow.

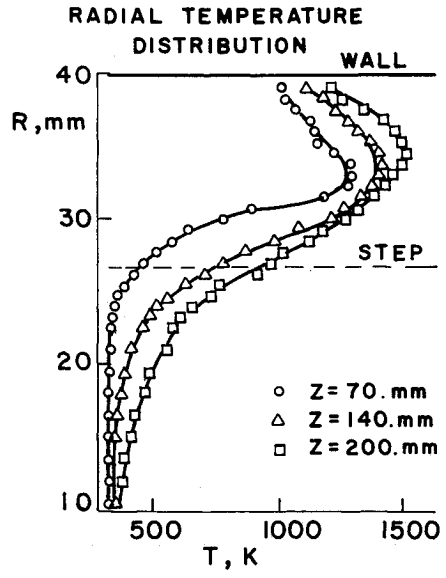

Fig. 8 Radial distribution of the gas temperature.

the radial distribution of the gas temperature for the specific conditions of air mass flow rate of 0.175 kg/s and fuel flow of 3.28 g/s. It shows the ring-like shape of the flame and the locus of the reaction region as those where temperature gradients exist.

Figure 9 demonstrates the radial distribution of the O_2 and CO_2 volume fractions. Here one sees also that the reaction zone is confined by the volume defined by the step. The droplet velocity distribution downstream of the nozzle (at 70 mm from the step, see Fig. 10) shows a fairly uniform profile without monotonic decay near the wall, ending at the region where there are no more droplets. The figure presents the radial distribution of the mean axial velocity and its turbulence intensity as well as the mean droplet diameter and its standard deviation (U_{max} = 53 m/s; $\bar{D}_{max}$ = 25 μm). It can be concluded that there is nearly no influence of the droplets on the average gas velocity. However, combustion accelerates significantly the flow to nearly one-and-a-half times its cold value.

V. Numerical Results

Two main case studies were performed for the isothermal two-phase flow and the reactive two-phase flow situation.

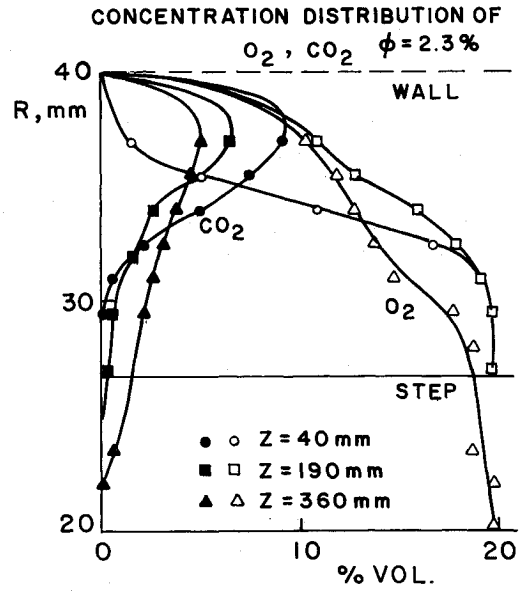

Fig. 9 Radial distribution of CO_2 and O_2 (% volume).

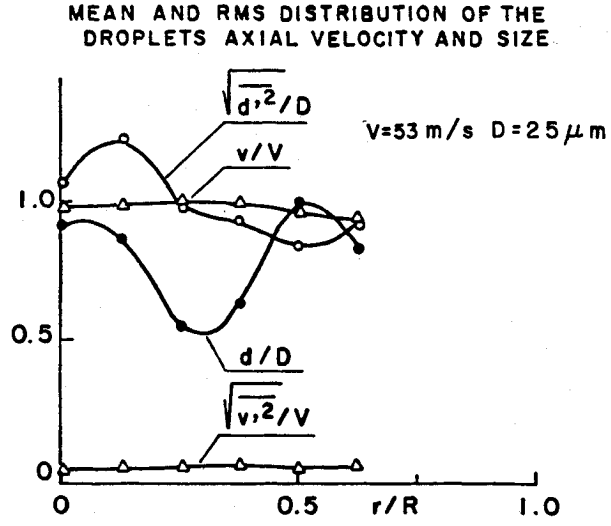

Fig. 10 Radial distribution of droplets properties in reactive flow: 1) normalized mean axial velocity; 2) turbulence intensity; 3) mean size; and 4) normalized variance of the droplets size.

Runs were performed using two types of hollow cone fuel injectors; a hypothetical one that is characterized by the Rosin Rammler droplet size distribution,[15] and the one that has the size distribution measured by the laser Doppler system. The parameters of the nozzles, which are the droplet size distribution, injection angle, and location of injection point at an axial distance, can serve as the initial conditions for the liquid-phase calculation.

In isothermal conditions, the influence of the type of injector was found not to be significant and both injectors exhibited the same flowfield pattern with recirculation regions of about nine times the step height. Contrary to the isothermal situation, in reactive flow the size distribution of droplets has significant influence on the flow pattern (see Fig. 11) through the distribution of energy release directly affected by fuel droplet evaporation rate and vapor diffusion. Figure 12 displays the contours of isotherms for the injector. The calculated trajectory of droplets of different sizes is shown in Fig. 13 for the practical spray nozzle. It shows the fast response of the small droplets to the gas flow and their fast evaporation rate. It is also clearly seen that there is no penetration of droplets into the recirculation zone. Figure 14 shows the contours of lines of equal fuel-to-air ratio. It should be noted that the

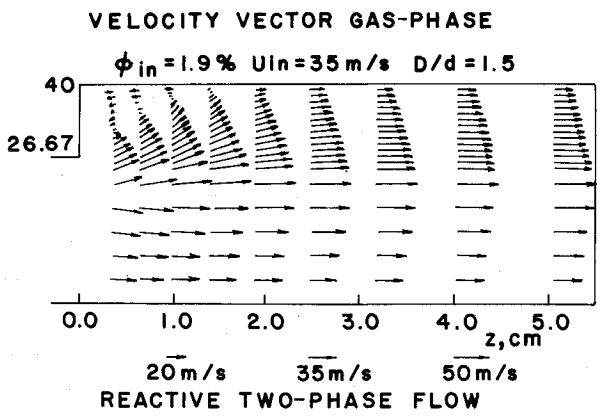

Fig. 11 The reactive flowfield with the experimental injector.

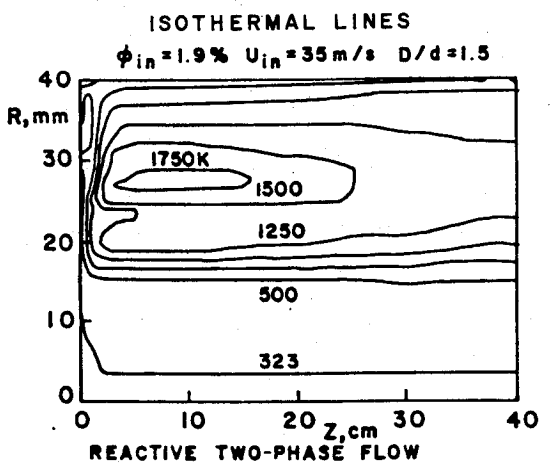

Fig. 12 Isotherms for reactive flow with the experimental injector.

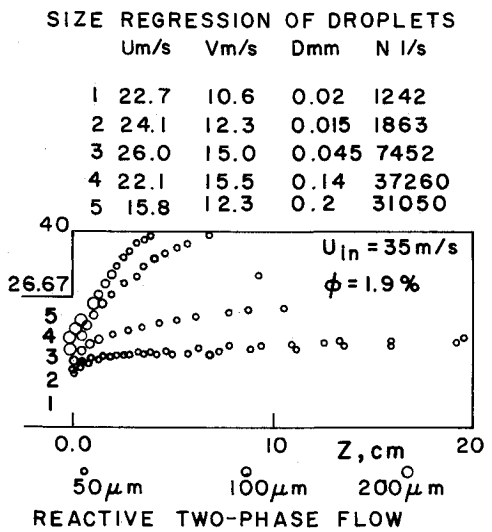

Fig. 13 Droplet trajectories.

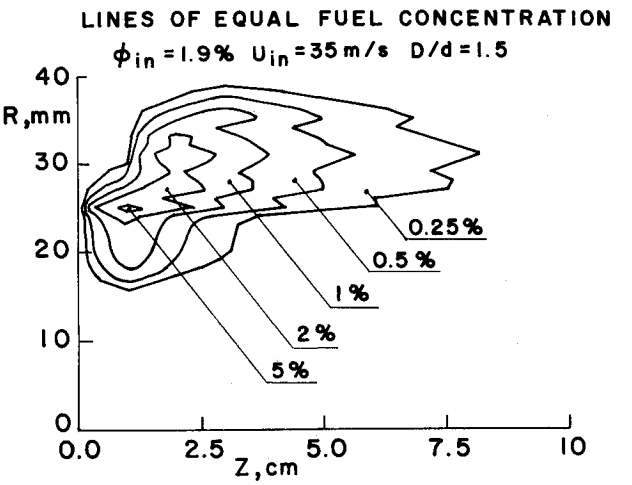

Fig. 14 Lines of equal fuel-to-air ratio for the experimental injector.

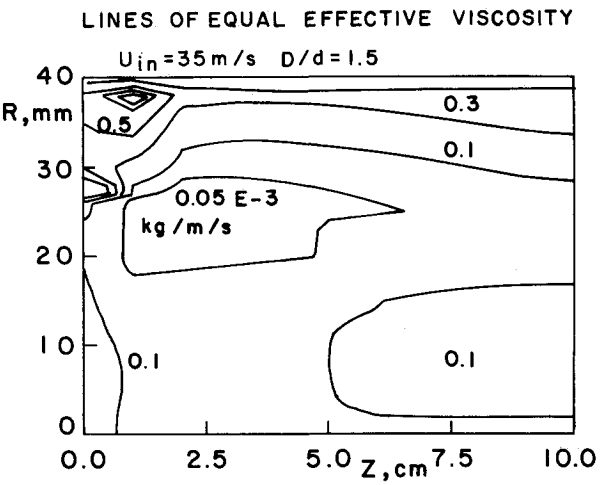

Fig. 15 Lines of equal effective viscosity.

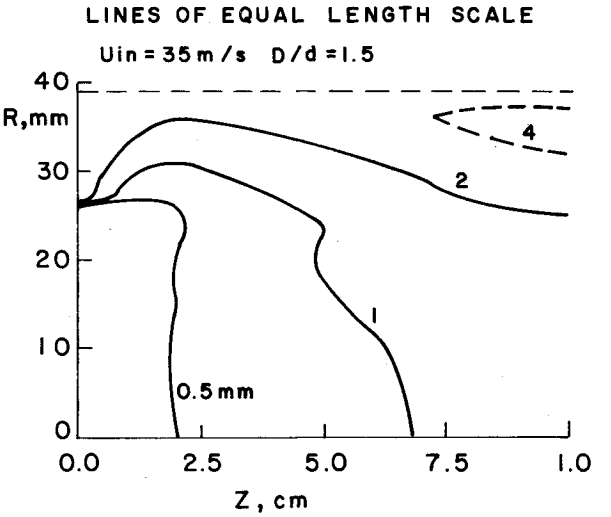

Fig. 16 Lines of equal length scale of the turbulence.

reaction is stable at regimes of fuel-to-air ratio of about 6.7% while the total equivalence ratio is about ⅓.

The viscous turbulence is proportional to the square of the turbulence energy divided by the dissipation. Figure 15 shows a big increase in the effective viscosity, up to ten times the core value. Figure 16 presents the distribution of the turbulence length scale, which is related to the mixing length. The larger the values, the slower the generation of combustion products. Hence, the regions where the mixing length is minimal will be those where combustion will take place on condition that the local equivalence ratio is appropriate. The dissipation length represents the time required for the molecular forces to absorb the energy of turbulence; hence, it can be an indication for the time required to mix the fuel vapor and air. Therefore, using the assumption that fuel and air exist in different vortices, combustion will occur only after a period of time equal to the lifetime of these vortices. Consequently the regions, where the dissipation length is sufficiently small and the fuel-to-air ratio is adequate, will be those where most of the combustion will occur. The regions of high

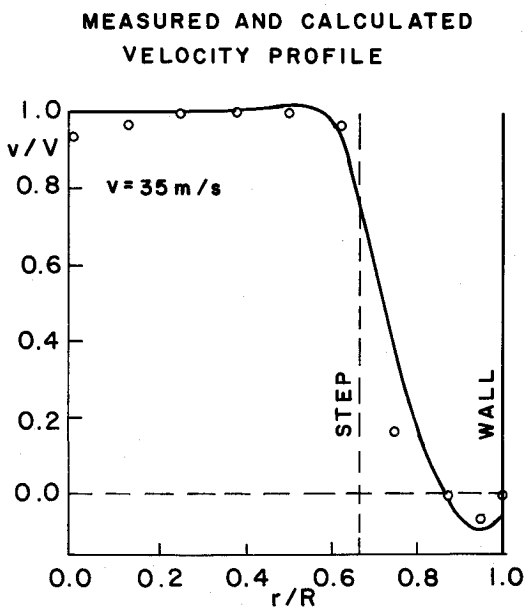

Fig. 17 Measured and calculated velocity profile.

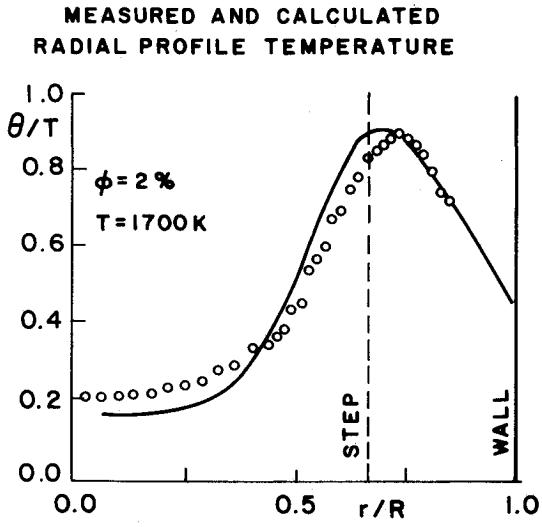

Fig. 18 Measured and calculated temperature profile.

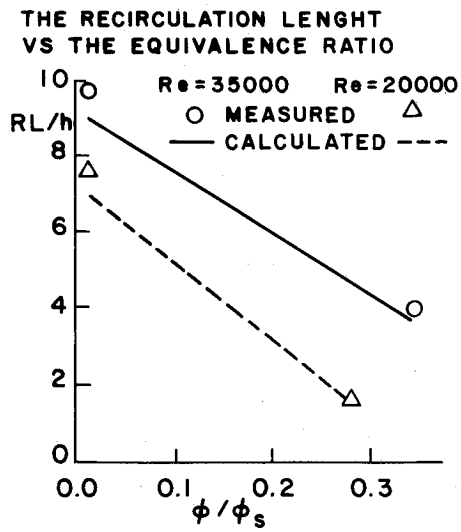

Fig. 19 The normalized length of the recirculation zone vs the equivalence ratio.

turbulent viscosity and small turbulence length scale are those where reaction will take place. It is seen that the recirculation zone is rich with fuel and the shear layer, which separates it from the core, is characterized by an equivalence ratio close to unity. Hence the flame will stabilize itself on the shear layer, which acts as a flameholder. Therefore, the geometry of this region (step height, reattachment point) defines the combustion volume and can serve as a parameter for combustion efficiency and intensity.

Comparison between experimental and numerical results is shown in Figs. 17–19. The radial distribution of the axial velocity is presented in Fig. 17 and shows fairly good agreement. A slight shift of the measured maximum temperature point towards the walls is observed in Fig. 18 and a variation as small as 10% is seen in the prediction of the recirculation length (Fig. 19) as a function of the fuel-to-air ratio for two different Reynolds numbers. It is interesting to note the sharp decrease of the recirculation length with fuel-to-air ratio; in our experiments it was also almost impossible to obtain stable combustion (corresponding to a very low recirculation length) at 30% equivalence ratio.

VI. Concluding Remarks

The recirculation zone plays a significant role in the performance of the dump combustor. It operates as a flameholder; hence its dimensions affect the combustion intensity and efficiency. Its dimensions are, however, defined by the characteristics of the two-phase flow together with the step height. Understanding the physical phenomena affecting the turbulent flow structure together with the droplets dynamics, which are responsible for the distribution of fuel vapor distribution, is a must if effective combustor design is required.

In cold flow, the recirculation length (from step to reattachment point) is linearly proportional to the step height and is related to the inlet Reynolds number. For turbulent flow ($Re \gtrsim 2000$), the normalized length maintains a fairly constant value. The radial pressure gradients have a significant effect on the reattachment of the flow and hence on the recirculation length. Hence back pressure, similar to that existing during combustion, will shorten its length. The momentum of the droplets has small effect on the (cold) airflow and consequently alters slightly its shape. Combustion causes acceleration of the flow in the hot regions and changes the whole structure of the flow. The large velocity gradients shorten eventually the recirculation zone, hence the strong dependence of the recirculation length on the total fuel-to-air ratio. The shear layer, separating the recirculation zone from the core, fulfills all requirements for stable chemical reaction. It is fuel rich, has low velocities, contains hot gas products, and has intensive mixing between fuel and air. Fuel injection has a significant influence on the combustion process as it controls the fuel vapor distribution in accordance with the droplets trajectories. It also affects the geometry of the shear layer due to the droplet momentum. Consequently, small droplets (small enough to evaporate before reaching the wall) with sufficient momentum and large spray angles will increase combustion intensity and shorten the combustor length required. However, a fuel-rich environment, which shortens significantly the recirculation length, can lead to flame blowout or to cold fuel-rich regions which eventually will be responsible for the creation of soot and drastic reduction in combustion efficiency. A consequent optimal dump combustor design will have a diameter ratio of above 2 ($D/d \gtrsim 2$) with a relative small inlet diameter (to avoid large combustor dimensions). It should have a total equivalence ratio close to one (≈ 0.85) with hollow cone spray nozzle and high inlet air velocities ($U \gtrsim 50$ m/s).

References

[1]Hsiao, C. C., Oppenheim, A. K., Ghoneim, A. F., and Chorin, A. J., "Numerical Simulation of a Turbulent Flame Stabilized Behind a Rearward-Facing Step," 20th Symposium (International) on Com-

bustion, The Combustion Inst., Ann Arbor, 1984, pp. 495–504.

[2]Nallasamy, M., "Computation of Confined Turbulent Coaxial Jet Flows," *Journal of Propulsion and Power*, Vol. 3, No. 3, 1987, pp. 263–268.

[3]Brum, R. D., and Samuelsen, G. S., "Two-Component Laser Anemometry Measurements of Nonreacting and Reacting Complex Flows in a Swirl Stabilized Model Combustor," *Experiments in Fluids*, Vol. 5, No. 2, 1987, pp. 95–102.

[4]Vanka, S. P., Craig, R. R., and Stull, F. D., "Mixing Chemical Reaction and Flowfield Development in Ducted Rockets," *Journal of Propulsion and power*, Vol. 2, No. 4, 1986, pp. 331–338.

[5]Stevenson, W. H., Thompson, H. D., and Luchik, T. S., "Laser Velocimeter Measurements and Analysis in Turbulent Flows with Combustion, Pt. I," AFWAL-TR-82-2076, 1982.

[6]Levy, Y., and Timnat, Y. M., "Two-Phase Flow Measurement Using a Modified Laser Doppler Anemometry System," *Progress in Astronautics and Aeronautics: Single and Multiphase Flows in an Electromagnetic Field*, Vol. 100, edited by H. Branover, P. S. Lykondis, and M. Mond, AIAA, New York, 1984, pp. 355–367.

[7]Bachalo, W. D., and Houser, M. J., "Phase/Doppler Spray Analyzer for Simultaneous Measurements of Drop Size and Velocity Distributions," *Optical Engineering*, Vol. 23, No. 5, 1984, pp. 583–590.

[8]Levy, Y., and Timnat, Y. M., "Laser Techniques for Measurements of Size and Velocity of Individual Drops Systems," *Israel Journal of Technology*, Vol. 23, 1986/7, Nos. 1–2, pp. 93–99.

[9]Durst, F., and Eliasson, B., "Properties of Laser Doppler Signals and Their Exploitation for Particle Size Measurements," *Proceedings of the LDA Symposium*, Copenhagen, 1975, pp. 457–477.

[10]Levy, Y., and Timnat, Y. M., "Diagnostics in Reacting Flows," *Progress in Astronautics and Aeronautics: Dynamics of Reactive Systems*, Vol. 113, edited by A. L. Kuhl, J. R. Bowen, J. C. Leyer, and A. Borisov, AIAA, New York, 1988, pp. 387–402.

[11]Jones, W. P., and Launder, B. E., "The Prediction of Laminarization with a Two-Equation Model of Turbulence," *International Journal of Heat and Mass Transfer*, Vol. 15, No. 2, 1972, pp. 301–304.

[12]Magnussen, B. F., and Hjertagger, B. H., "On Mathematical Modelling of Turbulent Combustion with Special Emphasis on Soot Formation and Combustion," 16th Symposium (International) on Combustion, The Combustion Inst., Cambridge, Mass., 1976, pp. 719–725.

[13]Crowe, C. T., Sharma, M. P., and Stock, D. E., "The Particle Source in Cell Model for Gas-Droplet Flows," *Journal of Fluids Engineering*, Vol. 99, No. 2, 1977, pp. 325–332.

[14]Laredo, D. Levy, Y., and Timnat, Y. M., "Two-Phase Flow Diagnostics in Reactive Systems," *Progress in Astronautics and Aeronautics: Liquid Metal Flows: Magnetohydrodynamics and Applications*, Vol. 111, edited by H. Branover, M. Monds, and Y. Unger, AIAA Series, Washington, D.C., 1988, pp. 605–618.

[15]Sturgess, G. J., Syed, S. A., and McManus, K. R., "Calculation of a Hollow-Cone Liquid Spray in a Uniform Airstream," *Journal of Propulsion and Power*, Vol. 1, No. 5, 1985, pp. 360–396.